Chronic Obstructive Pulmonary Diseases

9

Julia Ley-Zaporozhan, Ahmed F. Halaweish and Edwin J. R. van Beek

CONTENTS

KEY POINTS

MRI is becoming increasingly useful for imaging of lung structure and function, both in terms of airways imaging, assessment of ventilation and evaluation of lung perfusion and right heart function. This modality is highly versatile and capable of generating a range of inherent and exogenously introduced contrast mechanisms, while maintaining high resolution as well as incredible speed of data acquisition.
It is quite likely that MRI techniques will allow further evaluation of physiological and pathophysiological aspects of COPD, and this should ultimately lead to improved understanding and treatment of this heterogeneous diseases complex.

9.1 Introduction

Chronic obstructive pulmonary disease (COPD) is the fourth most common cause of death among adults (Rabe et al. 2007). COPD is characterized by incompletely reversible (usually progressive) airflow limitation, which is associated with an abnormal inflammatory response of the lung to noxious particles or gases. It is caused by a mixture of airway obstruction (obstructive bronchiolitis) and parenchymal destruction (emphysema), the relative contributions of which are variable (Rabe et al. 2007). Chronic bronchitis, or the presence of cough and sputum production for at least 3 months in each of 2 consecutive years, remains a clinically and epidemiologically useful diagnostic clas-

J. Ley-Zaporozhan, MD
Department of Pediatric Radiology, University Hospital Heidelberg, Im Neuenheimer Feld 430, 69120 Heidelberg, Germany

A. F. Halaweish
Department of Biomedical Engineering\Radiology, University of Iowa Hospitals and Clinics, 200 Hawkins Drive, Iowa City, IA 52242-1077, USA

E. J.R. van Beek, MD PhD
Department of Radiology, University of Iowa Hospitals and Clinics, 200 Hawkins Drive, Iowa City, IA 52242-1077, USA

sifying term. Pulmonary emphysema is a pathological term and is defined by the American Thoracic Society as an abnormal permanent enlargement of the air spaces distal to the terminal bronchioles, accompanied by the destruction of their walls. In a simplified way, obstructive airflow limitation leads to air-trapping with subsequent hyperinflation of the airspaces, which combined with inflammatory lung injury leads to destruction of the lung parenchyma. For severity assessment of COPD lung function tests, such as forced expiration volume in 1 s (FEV_1), FEV_1/FVC (forced vital capacity) and diffusing capacity for carbon monoxide (DLco) are used. However, pulmonary function tests only provide a global measure without any regional information and are not suitable for determination of structural abnormalities. Although extremely useful in clinical practice and for global management of patients, pulmonary function tests are known to be relatively insensitive to both early stages and small changes of manifest disease. Furthermore, pulmonary function tests are dependent upon the effort and compliance of the patient, and are difficult to reliably perform in young children. Chronic hyperinflation impacts on diaphragmatic geometry with subsequent dysfunction due to dissociation of the breathing mechanics. The disease also affects the pulmonary arteries: intimal thickening, smooth muscle hypertrophy and inflammation were described, which ultimately give rise to vascular remodeling (Szilasi et al. 2006). The direct vascular changes and hyperinflation lead to the precapillary type of pulmonary hypertension and pulmonary vascular flow disturbance (Rosenkranz 2007).

In contrast to pulmonary function tests, radiological imaging techniques may be able to differentiate the different components of obstructive lung disease on a regional basis, with the possibility of detecting early disease stages prior to the onset of severe symptoms. Computed tomography (CT) is the mainstay diagnostic modality in this field with emphasis on structural imaging of lung parenchyma and airways. Magnetic resonance imaging (MRI) has the potential to provide regional information about the lung without the use of ionizing radiation, but is hampered by several challenges: the low amount of tissue relates to a small number of protons leading to low signal, countless air-tissue interfaces cause substantial susceptibility artifacts and last but not least, respiratory and cardiac motion. In several lung diseases, such as tumors, the amount of protons or the blood volume is actually increased and motion is reduced, which provides better pre-conditions for MRI. In obstructive pulmonary disease, however, there are no facilitating disease-related effects as there is loss of tissue and reduced blood volume due to hypoxic vasoconstriction and the degree of hyperinflation has a negative correlation with the MR signal (Ley-Zaporozhan et al. 2008). The depiction of the airways by MRI is certainly limited to the central bronchi. Fortunately, MRI has shown significant potential beyond the mere visualization of structure by providing comprehensive information about "function", such as perfusion, hemodynamics, ventilation and respiratory mechanics.

9.2 Parenchyma

The most frequently utilized sequences in MRI of COPD are acquired in a single breath-hold. For fast T2-weighted imaging, single shot techniques with partial-Fourier acquisition (HASTE) or ultrashort TE (UTSE) are recommended (Figs. 9.1 and 9.2). The T2-weighted HASTE sequence in coronal and/or axial orientation allows for the depiction of pulmonary infiltrates, inflammatory bronchial wall thickening and mucus collections. T1-weighted 3D gradient echo sequences, such as VIBE, are suitable for the assessment of the mediastinum and common nodular lesions. The intravenous application of contrast material markedly improves the diagnostic yield of T1 weighted sequences by a clearer depiction of vessels, hilar structures and solid pathologies. A major goal in inflammatory obstructive airway disease is to differentiate inflammation within the wall from muscular hypertrophy, edema and mucus collection which cannot be achieved by CT, but can be addressed by the use of T1- and T2-weighted images as well as contrast enhancement (Ley-Zaporozhan et al. 2008).

The extent of hyperinflation and hypoxic vasoconstriction is directly associated with the loss of signal (Bankier et al. 2004). Thus, until now, MRI of the pulmonary parenchyma has only been successfully applied to diseases with an increase of tissue and resultant signal. While emphysematous destruction can hardly be diagnosed by a loss of signal, it is much easier to detect hyperinflation just by the size or volume of the thorax. In a recent study, it was shown that the change of parenchymal signal intensity measured by MRI at inspiration and expiration correlates with FEV_1 ($r = 0.508$) and might warrant further studies as a predictor of airflow obstruction (Iwasawa et al. 2007).

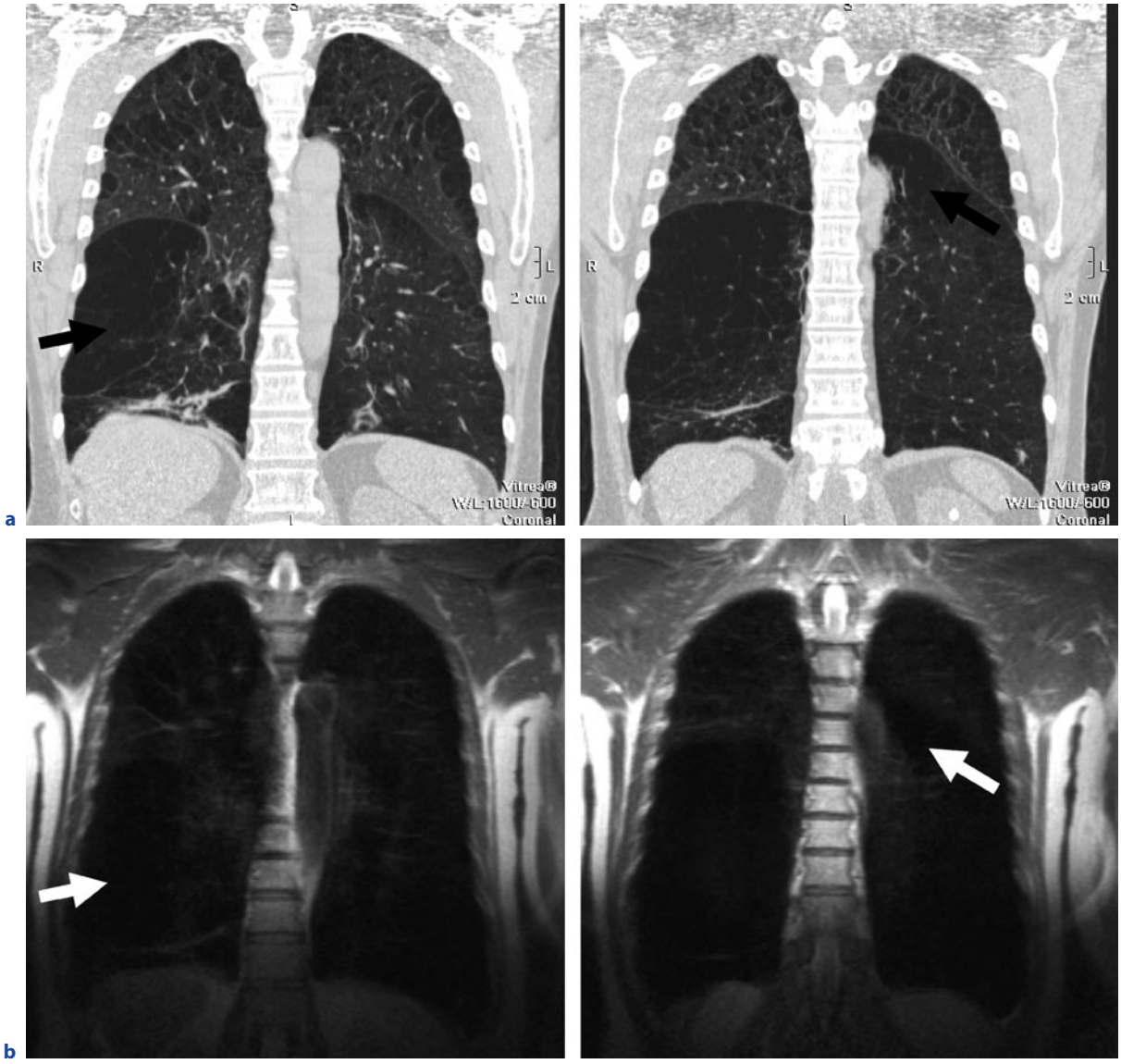

Fig. 9.1a,b. Coronal CT reformats (**a**) and corresponding coronal T2 weighted (HASTE) images (**b**): severe emphysema with predominance of the right lower lobe on CT corresponds to a loss of MR signal (*arrows*) reflecting destruction of the parenchyma and paucity of pulmonary vasculature of the pulmonary vasculature

Fig. 9.2. Coronal T2 weighted (HASTE) image shows the typical flattening of the diaphragm in emphysema

9.3 Airways

Several pathological studies have shown that a major site of airway obstruction in patients with COPD is in airways smaller than 2 mm internal diameter (Hogg et al. 2004). The 2-mm airways are located between the 4th and the 14th generation of the tracheobronchial tree. Airflow limitation is closely associated with the severity of luminal occlusion by inflammatory exudates and thickening of the airway walls due to remodeling. Severe peripheral airflow obstruction can also affect the proximal airways from subsegmental bronchi to the trachea.

For assessment of tracheal instability MR cine acquisitions during continuous respiration or forced expiration are recommended (Heussel et al. 2004). The depiction of airway dimensions and thickness of the airway walls by MRI under physiological conditions is limited to the central bronchi. For depiction of the bronchiectasis high spatial resolution is essential. By using a 3D volume interpolated gradient echo sequence (VIBE) with a voxel size of approximately 0.9 × 0.88 × 2.5 mm a sensitivity of 79% and a specificity of 98% regarding the visual depiction of bronchiectasis was shown compared to CT (Biederer et al. 2003).

9.4 Respiratory Dynamics

Respiration is the result of the complex interaction between chest wall and diaphragm motion, and it can be visualized by 2D or 3D dynamic MR techniques (Cluzel et al. 2000; Plathow et al. 2004, 2005). For data acquisition time resolved techniques are used which can be based on FLASH or trueFISP sequences. This allows for a high temporal resolution down to 100 ms per frame.

Hyperinflation of the lung severely affects diaphragmatic geometry with subsequent reduction of the mechanical properties, while the effects on the mechanical advantage of the neck and rib cage muscles are less pronounced (Decramer 1997). The common clinical measurements of COPD do not provide insights into how structural alterations in the lung lead to dysfunction in the breathing mechanics, although treatments such as lung volume reduction surgery (LVRS) are thought to improve lung function by facilitating breathing mechanics and increasing elastic recoil (Henderson et al. 2007).

In contrast to normal subjects with regular, synchronous diaphragm and chest wall motion, dynamic MRI in patients with emphysema frequently showed reduced, irregular or asynchronous motion, with a significant decrease in the maximum amplitude and the length of apposition of the diaphragm (Suga et al. 1999). In some patients the ventral portion of the hemidiaphragm moved downward at MRI while the dorsal part moved upward like a seesaw (Iwasawa et al. 2000). The paradoxical diaphragmatic motion correlated with hyperinflation, although severe hyperinflation tended to restrict both normal and paradoxical diaphragmatic motion (Iwasawa et al. 2002). After LVRS, patients showed improvements in diaphragm and chest wall configuration and mobility at MRI (Suga et al. 1999). Ultrafast dynamic proton MRI was shown to be able to demonstrate the rapid volume changes observed during forced vital capacity maneuver (Fig. 9.3) and correlated closely with pulmonary function tests, but with the added advantage of providing regional information on changes in lung volumes during this procedure (Eichinger et al. 2007; Swift et al. 2007).

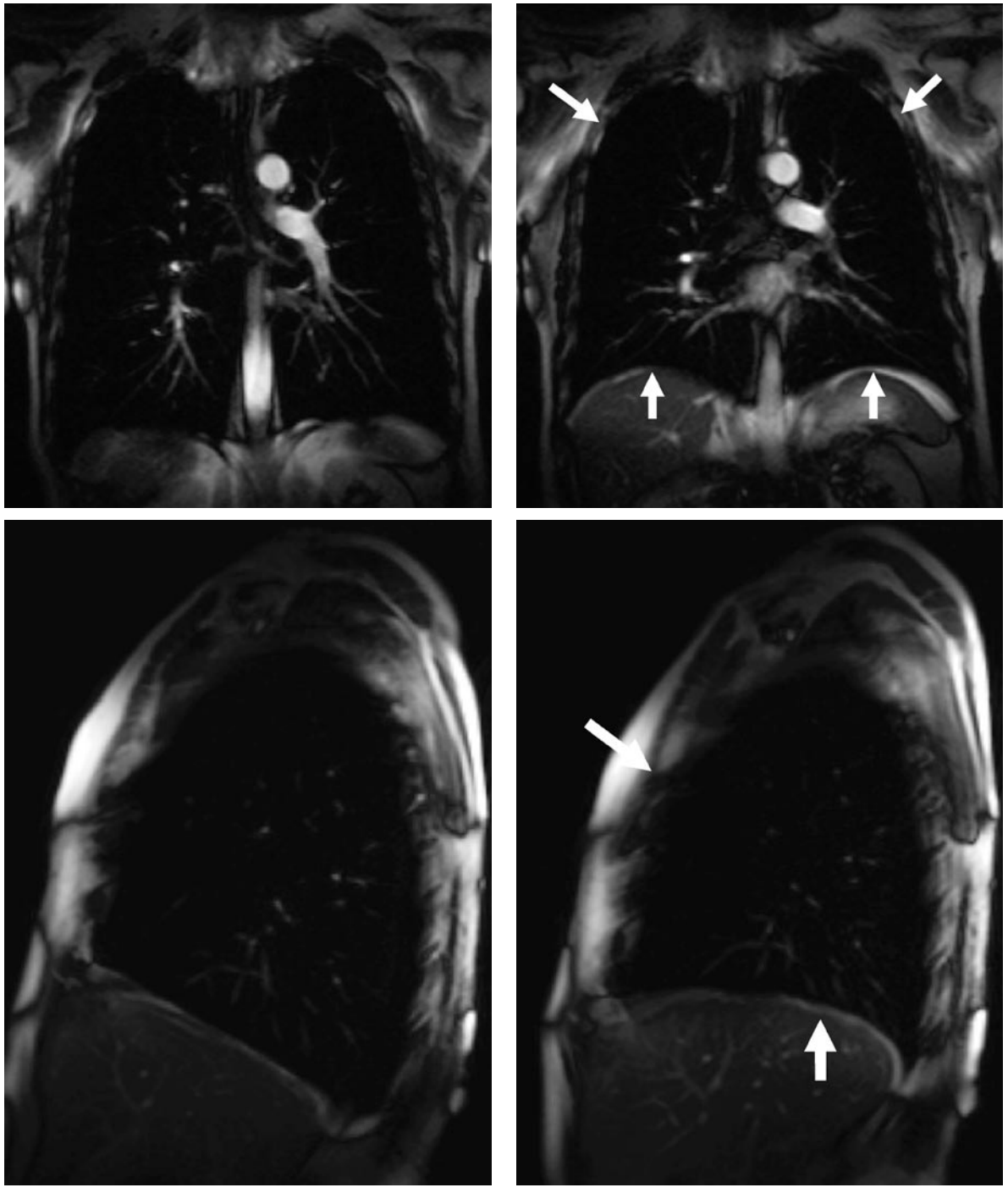

Fig. 9.3a–d. Coronal and sagittal MR images taken from a dynamic series acquired in a COPD patient during forced expiration reflecting maximum inspiration (**a,c**) and maximum expiration (**b,d**) shows motion of the diaphragm and thoracic wall (*arrows*)

9.5 Ventilation

As sufficient gas exchange depends on matched perfusion and ventilation, assessment of regional ventilation is important for the diagnosis and evaluation of pulmonary emphysema. Currently, the most established method for imaging regional lung ventilation are nuclear medicine studies using krypton-81m (Kr-81m), xenon-133 (Xe-133), radiolabeled aerosol (Technegas) and technetium-99m (Tc-99m)-labeled diethylentriaminepentaacetic acid (DTPA). The utility of nuclear medicine in pulmonary diseases has been well documented. However, these techniques are hampered by low spatial resolution and the necessity of inhalation of radioactive tracers, while 3D (SPECT) imaging will require approximately 20 min of imaging time, thus limiting the diagnostic power of the technique.

Although PFTs and nuclear medicine imaging have been established as the most common and reliable pulmonary function techniques, others such as contrast enhanced proton studies and hyperpolarized noble gas MRI are strong contenders in the functional imaging race, as they provide a rapid, high resolution regional quantification of disease progress and onset without the need for ionizing radiation tracers.

9.5.1 Oxygen-Enhanced Imaging

Oxygen-enhanced MRI requires no special scanner hardware, is easy to use and the overall material costs are low in comparison with noble gas imaging. The main idea behind this technique is to utilize the paramagnetic properties of inhaled oxygen (O_2) to obtain information regarding the pulmonary blood flow volume and integrity of the lung parenchyma (see Sect. 4.4). Several investigators reported that oxygen enhanced MRI could demonstrate regional ventilation (Edelman et al. 1996; Loffler et al. 2000; Ohno et al. 2001). The technique of oxygen-enhanced MRI has been successfully applied in volunteers; the translation into clinical examination however is difficult. Only few studies have successfully applied oxygen-enhanced MRI to patients with pulmonary diseases in a clinical setting. One of the reasons might be that the use of high oxygen concentrations (15 L/min) may not be without risk in patients with severe COPD.

In some basic measurements it was shown, that the T1 of the lung parenchyma is significantly shorter in patients with emphysema than in volunteers (Stadler et al. 2008). In a preliminary study an inhomogeneous and weak signal intensity increase after application of oxygen was observed, compared to healthy volunteers (Muller et al. 2002). Ohno et al (2003) demonstrated that regional changes in ventilation as observed in oxygen-enhanced MR reflected regional lung function. The maximum mean relative enhancement ratio correlated with the diffusion capacity for carbon monoxide ($r^2 = 0.83$), while the mean slope of relative enhancement was strongly correlated with the FEV_1 ($r^2 = 0.74$) and the maximum mean relative enhancement with the high-resolution CT emphysema score ($r^2 = 0.38$). Recent work also suggests that the simple administration of pure oxygen induces the pulmonary arteries to dilate resulting in an increase of pulmonary blood volume and a consecutive increase in signal intensity (Ley et al. 2007).

9.5.2 Hyperpolarized Noble Gas Imaging

Over the past decade hyperpolarized noble gas MRI using ^{3}Helium and ^{129}Xenon was developed to improve imaging of pulmonary structure, ventilation, dynamics and oxygen uptake. ^{3}Helium has become the most widely used gas for these studies as it provides higher signal-to-noise ratios than ^{129}Xenon, due to its intrinsic gyromagnetic ratio, and its confinement to the airways and airspaces without dissolving into the surrounding tissue and bloodstream (van Beek et al. 2004). Areas with ventilation defects caused by airway obstruction and emphysema represent the only limitation because they cannot be assessed due to lack of the tracer gas entering these areas. Thus, there is almost no information about these affected lung regions. Overall, the intrinsic high cost of these noble gases, the need for laser-induced hyperpolarization hardware, and the need for non-proton imaging hardware and software remain the major drawbacks of this technology on its way to broader clinical applications.

9.5.2.1 Static Ventilation

Airflow obstruction leads to a reduced level of ^{3}Helium in the distal lung regions allowing for sensitive detection of ventilation abnormalities (Figs. 9.4 and 9.5) (Kauczor et al. 1996). In healthy smokers with normal lung function even subtle ventilation defects were visualized demonstrating the high sensitivity of the technique (Guenther et al. 2000). The volume of ventilated

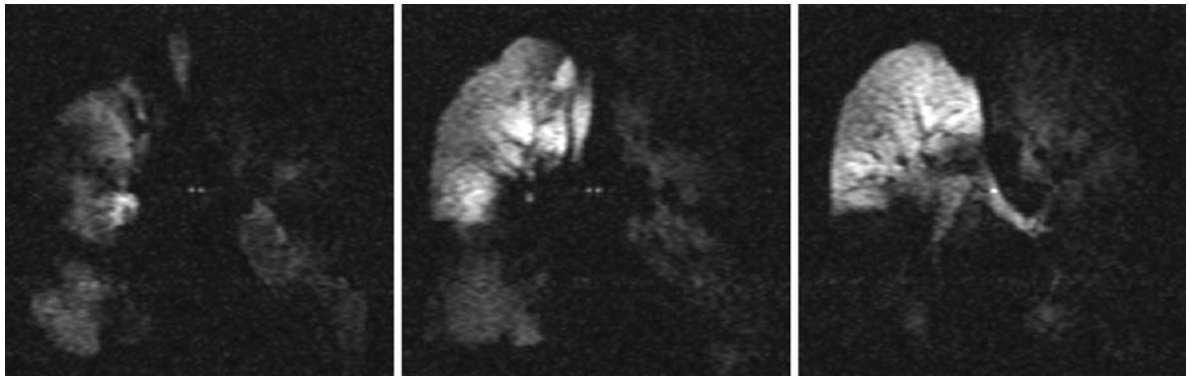

Fig. 9.4. MR ventilation images using hyperpolarized ^{3}Helium gas of a patient suffering from alpha1-antitrypsin-deficiency: good ventilation of the right upper lobe and large wedge-shaped ventilation defects in all remaining lung areas

Fig. 9.5. MR ventilation images using hyperpolarized ^{3}Helium gas of a patient suffering from COPD: focal and wedge-shaped ventilation defects in all parts of the lung

lung areas on ^{3}He-MRI correlated well with vital capacity (r = 0.9) and the amount of non-emphysematous volume on CT (r = 0.7) in patients with severe emphysema following single lung transplantation (Zaporozhan et al. 2004). Ventilation defects correlated well with the parenchymal destruction assessed by HRCT in patients with severe emphysema following single lung transplantation (Gast et al. 2002). Quantification of ventilatory impairment can be achieved by automatic segmentation of the lung allowing for precise pre- and post-therapeutic comparison of ventilation (Ray et al. 2003). In addition, a proton-3-He subtraction method has been shown to be reproducible and easily implementable, allowing for sensitive quantification of ventilated lung volumes (Woodhouse et al. 2005).

9.5.2.2 Dynamic Assessment

^{3}Helium MR imaging with high temporal resolution via ultra-fast Echo-planar (EPI), Gradient-echo and interleaved spiral sequences allows for the visualization and assessment of the various inspiratory and expiratory phases of respiration. The instantaneous visualization of the bolus movement leads to a direct evaluation of the regional distribution of ventilation throughout the lungs, which may be quantified using a regional assessment (Lehmann et al. 2004). Evaluation of the overall usefulness of the technique has shown considerable airflow abnormalities in diseased lung states and normal respiration stages in normal lungs (Salerno et al. 2001; Wild et al. 2003). Normal respiration can be described by a rapid and homogenous distribution of the gas throughout the lung, whereas in diseased lungs, the airflow is inhomogeneous due to factors such as airway blockages and reduced lung compliance, leading to interspersed ventilation defects (Fig. 9.6). The observed ventilation defects vary from reduced inflow to air trapping as observed in the later phases of the respiratory cycle, which are more markedly visualized in subjects with CT proven centrilobular emphysema (Gast et al. 2003; Gierada et al. 2000; Wild et al. 2003).

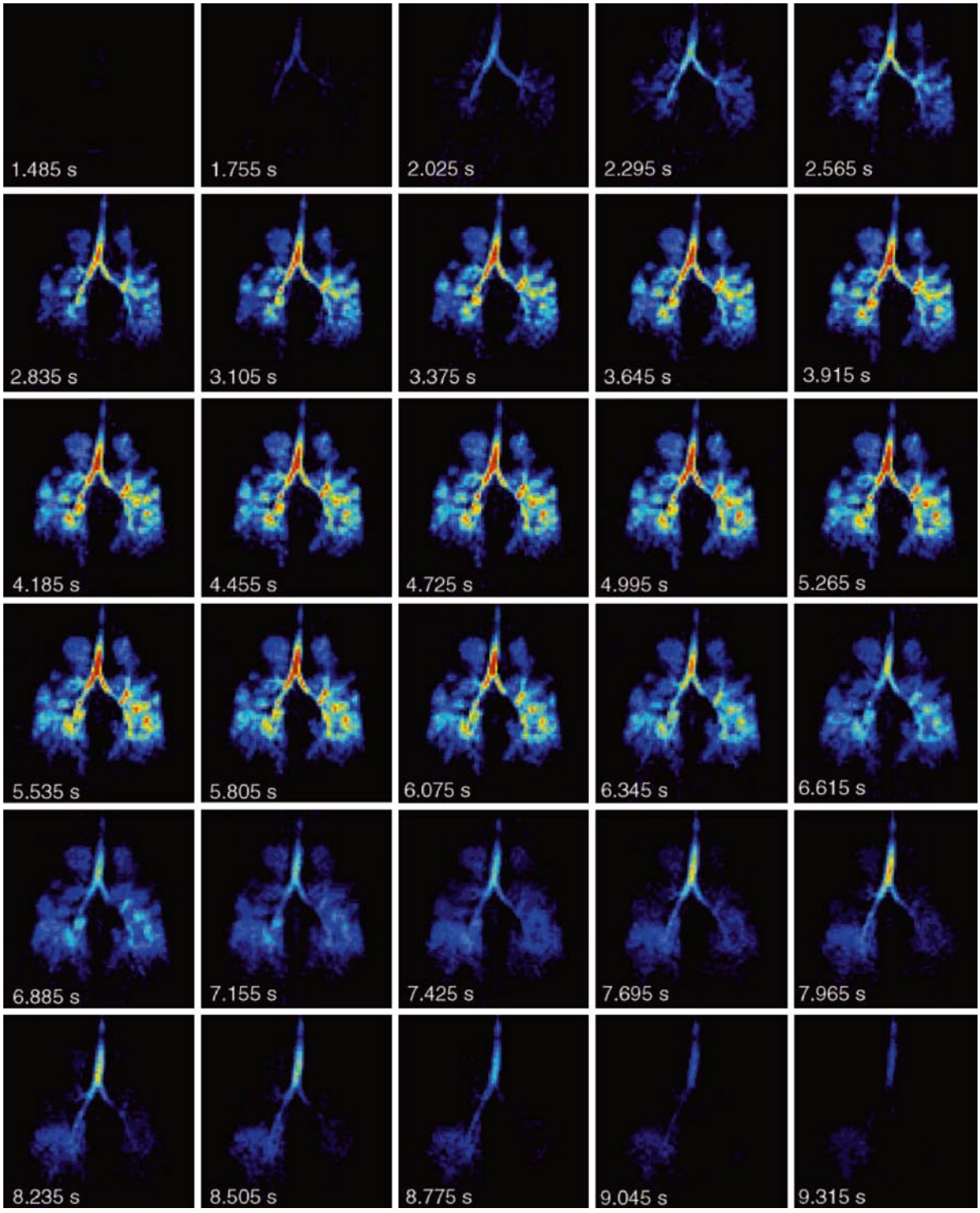

Fig. 9.6. Dynamic MR ventilation images using hyperpolarized ^{3}Helium gas from a COPD patient showing regions of ventilation obstruction in both lungs, particularly in the upper lobes and a delayed emptying/depolarization of gas in the lower left lobe, which could be indicative of air trapping (reprinted with permission from van Beek et al 2004)

9.5.2.3 ^{3}Helium Apparent Diffusion Coefficient (ADC)

The high diffusion coefficient of ^{3}Helium gas makes it very suitable for the evaluation of the lung microstructure, connecting pores and pathways, leading to an overall assessment of the integrity and size of such structures. The ADC is a reflection of the restricted diffusion of ^{3}Helium gas in a normal airway system due to the relatively small size of airways in relation to the diffusivity of the gas.

Similar to all other ^{3}Helium techniques, the ADC is accomplished throughout one single breath hold, where a series of images is acquired and evaluated on a pixel-by-pixel basis. The introduction of the additional gradients into the sequences allows the monitoring of diffusion through signal decay incurred by motion of the helium molecules, thus creating a map of diffusion values representing the regional and global integrity of the lungs.

ADC maps of normal healthy volunteers have shown to be homogenous and uniform. On the other hand, in emphysematous subjects ADC maps were non-uniform and contained larger diffusion values. This non-uniformity of the ADC values correlates well with the nature of the disease, where the degree and location of destruction varies throughout the lung (Conradi et al. 2005; Ley et al. 2004b; Salerno et al. 2002). The ability to distinguish between normal and emphysematous lungs reflects the overall power of determining and quantifying airway enlargement along with tissue destruction. The mean ADC for emphysema patients (0.452 cm^2/s) was found to be significantly larger ($p < 0.002$) than for normal volunteers (0.225 cm^2/s) (Salerno et al. 2002). In other studies, mean ADC values of emphysema patients were as low as 0.24 cm^2/s and as high as 0.55 cm^2/s (Conradi et al. 2005; Swift et al. 2005). These values and their standard deviations correlated good ($r = -0.6$) with predicted percentages of FEV1 (Swift et al. 2005). This wide distribution of ADC values for the emphysema population can be attributed to the variability in airspace size and morphological alterations of the distal airspaces caused by the disease. The reproducibility of these ADC measures has been demonstrated to be very high, within 5% for consecutive scans (Morbach et al. 2005).

9.6 Pulmonary Perfusion

Perfusion and ventilation are normally in balance, with hypoxic vasoconstrictive response providing a method to optimize lung function. In patients with COPD, ventilation is impaired due to airway obstruction and parenchymal destruction, leading to perfusion being moved to better ventilated lung regions or shunting of blood (moving through the lungs without reaching a capillary bed for gas exchange) (Moonen et al. 2005). The reduction of the pulmonary vascular bed is related to the severity of parenchymal destruction (Thabut et al. 2005); however the distribution of perfusion does not necessarily match parenchymal destruction (Ley-Zaporozhan et al. 2007; Sandek et al. 2002). Conventional radionuclide perfusion scintigraphy has been used to assess these abnormalities, but it has substantial limitations with respect to spatial and temporal resolution. A superior technique is SPECT, which is rarely used as it is rather time consuming and not routinely applied. Inflammation appears to play a critical role in the maintenance of the hypoxic vasoconstrictive response, and PET studies with endotoxin challenge have shown that this response is shut off when inflammation and lung injury occur (Gust et al. 1998; Schuster and Marklin 1986).

The basic principle of contrast-enhanced perfusion MRI is a dynamic acquisition during and after an intravenous bolus injection of a paramagnetic contrast agent. With the introduction of parallel imaging techniques, 3D perfusion imaging with a high spatial and temporal resolution, as well as an improved anatomical coverage and z-axis resolution can be acquired (Fink et al. 2004, 2005; Ley et al. 2004a). These data sets are also well suited for high quality multiplanar reformats. Due to high spatial resolution, detailed analysis of pulmonary perfusion and precise anatomical localization of the perfusion defects on a lobar and even segmental level can be performed (Fig. 9.7). Quantitative values for pulmonary perfusion can be obtained by applying the principles of indicator dilution techniques. The quantitative indices, such as mean transit time (MTT), pulmonary blood volume (PBV), and blood flow (PBF), are derived from the time intensity curve, defined by the dynamic series of perfusion MR images (also see Chap. 3).

MR perfusion allows for a high diagnostic accuracy in detecting perfusion abnormalities (Fink et al. 2004; Sergiacomi et al. 2003). Furthermore, MR perfusion ratios correlate well with radionuclide perfusion scintigraphy ratios (Molinari et al. 2006; Ohno et al. 2004a).

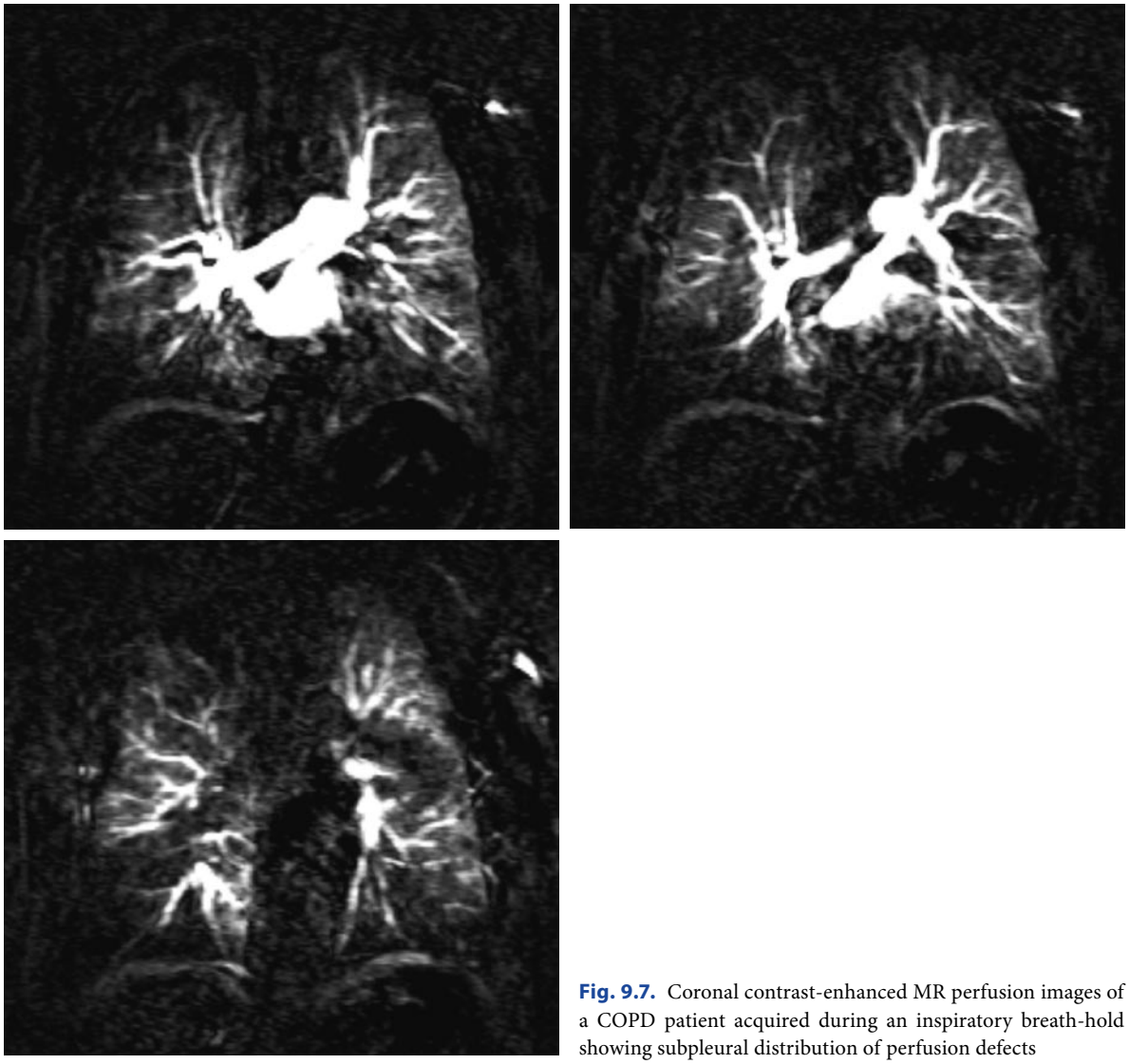

Fig. 9.7. Coronal contrast-enhanced MR perfusion images of a COPD patient acquired during an inspiratory breath-hold showing subpleural distribution of perfusion defects

Lobar and segmental analysis of the perfusion defects can be achieved (Ley-Zaporozhan et al. 2007).

The perfusion abnormalities in COPD clearly differ from those caused by vascular obstruction. While wedge shaped perfusion defects occur in embolic vascular obstruction, a low degree of contrast enhancement is generally found in patients with COPD/emphysema (Amundsen et al. 2002; Morino et al. 2006). Furthermore, the peak signal intensity is usually reduced. These features allow for easy visual differentiation. In patients with COPD, the quantitative evaluation of 3D perfusion showed that the mean PBF, PBV and MTT were significantly decreased, and these changes showed a very heterogeneous distribution (Ohno et al. 2004b). It was discussed that patients with emphysema have hypoxia as well as destruction of lung parenchyma and fewer alveolar capillaries. This causes increased pulmonary arterial resistance and, secondarily to adaptive processes, pulmonary hypertension and right ventricular dysfunction. Ultimately, this results in decreased pulmonary blood flow in addition to heterogenous perfusion and decreased PBV. MTT is determined by the ratio between PBV and PBF. The results suggested that MTT is significantly decreased, reflecting a larger degree of decrease in PBV compared with PBF, with concomitant increased heterogeneity of regional PBV. Obviously, accurate quantitative measurements of such regional changes are important for improved understanding of lung pathophysiology in COPD.

9.7 Hemodynamics

Assessment of right ventricular function is important, as this is where the strain of perfusion obstruction and pulmonary hypertension eventually leads to the demise of the patient. MRI is able to assess right ventricular function through either phase contrast flow measurements in the pulmonary trunk (Fig. 9.8) or by short axis cine-acquisition of the right ventricle (Gatehouse et al. 2005; Vonk-Noordegraaf et al. 2005). Thus, early changes of the complex geometry of the right ventricular wall and chamber volume can be accurately measured.

Although pulmonary hypertension and cor pulmonale are rather common sequelae of COPD, the direct mechanism remains unclear (Szilasi et al. 2006). In COPD patients the pulmonary vessels show a reduced capacity for vessel dilatation due to a defect in synthesis and/or release of nitric oxide. Prior to the onset of clinical symptoms patients exhibit signs of vascular bed obstruction and elevated pulmonary artery pressure including main pulmonary artery dilatation. Pulmonary hypertension is most often mild to moderate (mean pulmonary artery pressure in the range 20–35 mmHg), but it may worsen markedly during acute exacerbations, sleep and exercise. Assessment of the pulmonary arterial pressure is necessary in COPD patients for at least two reasons: such patients have a poor prognosis; and they need adequate treatment that might include pulmonary vasodilators.

It has been demonstrated by several studies that the level of pulmonary hypertension has a prognostic

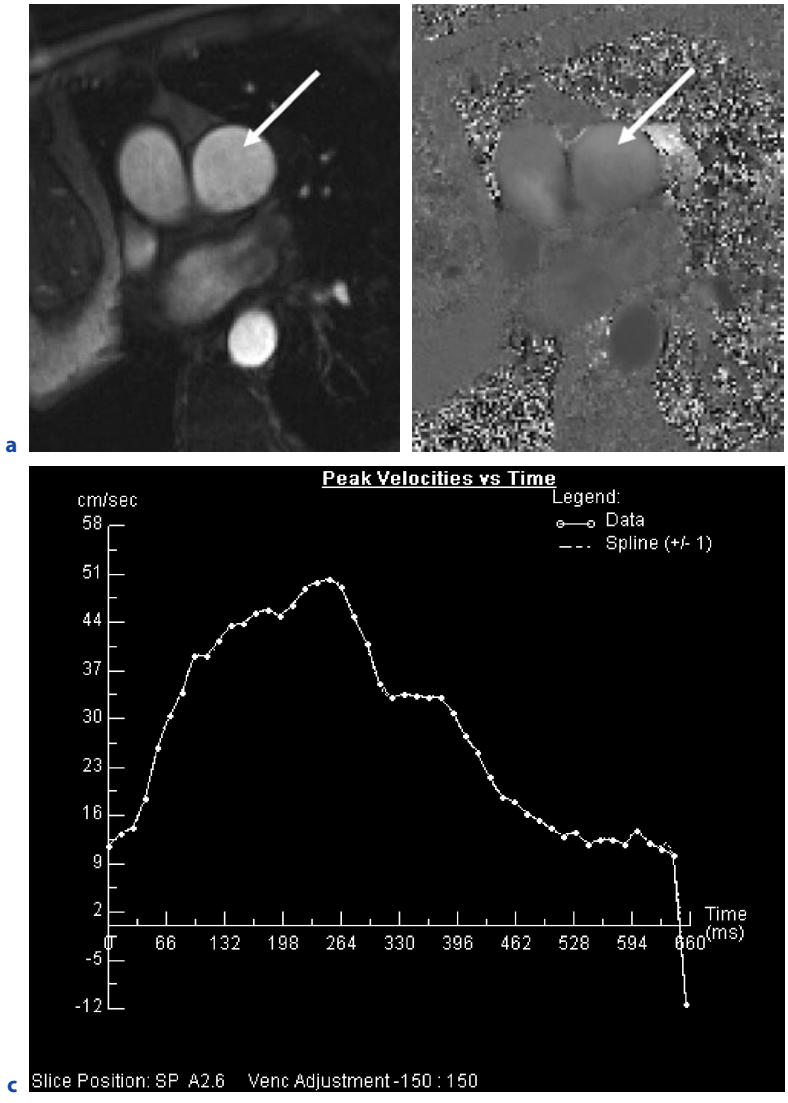

Fig. 9.8a–c. Quantitative flow measurement of pulmonary blood flow. Magnitude (**a**) and velocity encoded (**b**) image of the pulmonary trunk (*arrow*). Results of peak velocity over time (**c**) show the prolonged increase of velocity at the beginning of the systolic phase followed by an abnormal plateau during diastole

impact in COPD patients. In one of these studies, the 5-year survival rates were 50% in patients with mild (20–30 mmHg), 30% in those with moderate-to-severe (30–50 mmHg), and 0% in the small group (n = 15) of patients with very severe pulmonary hypertension (> 50 mmHg). Thus, severe pulmonary hypertension carries a poor prognosis, and this has also been observed in COPD patients receiving long-term oxygen therapy (Weitzenblum and Chaouat 2005).

Initially, a rise in pulmonary blood pressure leads to pulmonary artery dilatation while right ventricular performance is usually maintained. Evaluation of the right ventricle and pulmonary blood flow by echocardiography is difficult in patients with emphysema as the acoustic window is limited. Therefore, MRI has been used for imaging the right ventricle, and a loose correlation between increased right ventricular mass and the severity of emphysema was demonstrated (Boxt 1996).

In COPD patients with hypoxemia, increased right ventricular volumes, decreased right ventricular function, and impaired left ventricular diastolic function were shown (Budev et al. 2003). In a study by Vonk-Nordegraaf et al. (1997) the right ventricular mass and ejection fraction in 25 clinically stable, normoxic COPD patients with emphysema were analyzed. The position of the heart appeared rotated and shifted to a more vertical position in the thoracic cavity due to hyperinflation of the lungs with an increase of the retrosternal space. The right ventricular wall mass was significantly higher (68 g) in the patient group compared to healthy volunteers (59 g). The right ventricular ejection fraction was unchanged (53%). In another study from the same group, structural and functional cardiac changes in COPD patients with normal P_aO_2 and without signs of right ventricular failure were evaluated. Compared to healthy volunteers, there were no indications of pulmonary hypertension. However the end-systolic and end-diastolic volumes of the right ventricle were significantly reduced (with normal ejection fraction), the right ventricular mass was significantly elevated while the left ventricular mass was within normal limits. The authors conclude that concentric right ventricular hypertrophy is the earliest sign of right ventricular pressure increase in patients with COPD. This structural adaptation of the heart initially does not alter right and left ventricular systolic function (Vonk-Noordegraaf et al. 2005). As this is the only study so far in patients with mild emphysema, no strong conclusions can be drawn from this first description of the early adaptation mechanisms of the right ventricle in patients with normoxemia or mild hypoxemia and the consequences of any structural changes on right and left ventricular function.

References

Amundsen T, Torheim G, Kvistad KA et al. (2002) Perfusion abnormalities in pulmonary embolism studied with perfusion MRI and ventilation-perfusion scintigraphy: an intra-modality and inter-modality agreement study. J Magn Reson Imaging 15:386–394

Bankier AA, O'Donnell CR, Mai VM et al. (2004) Impact of lung volume on MR signal intensity changes of the lung parenchyma. J Magn Reson Imaging 20:961–966

Biederer J, Both M, Graessner J et al. (2003) Lung morphology: fast MR imaging assessment with a volumetric interpolated breath-hold technique: initial experience with patients. Radiology 226:242–249

Boxt LM (1996) MR imaging of pulmonary hypertension and right ventricular dysfunction. Magn Reson Imaging Clin N Am 4:307–325

Budev MM, Arroliga AC, Wiedemann HP et al. (2003) Cor pulmonale: an overview. Semin Respir Crit Care Med 24:233–244

Cluzel P, Similowski T, Chartrand-Lefebvre C et al. (2000) Diaphragm and chest wall: assessment of the inspiratory pump with MR imaging-preliminary observations. Radiology 215:574–583

Conradi MS, Yablonskiy DA, Woods JC et al. (2005) 3He diffusion MRI of the lung. Acad Radiol 12:1406–1413

Decramer M (1997) Hyperinflation and respiratory muscle interaction. Eur Respir J 10:934–941

Edelman RR, Hatabu H, Tadamura E et al. (1996) Noninvasive assessment of regional ventilation in the human lung using oxygen-enhanced magnetic resonance imaging. Nat Med 2:1236–1239

Eichinger M, Tetzlaff R, Puderbach M et al. (2007) Proton magnetic resonance imaging for assessment of lung function and respiratory dynamics. Eur J Radiol 64:329–334

Fink C, Puderbach M, Bock M et al. (2004) Regional lung perfusion: assessment with partially parallel three-dimensional MR imaging. Radiology 231:175–184

Fink C, Ley S, Kroeker R et al. (2005) Time-resolved contrast-enhanced three-dimensional magnetic resonance angiography of the chest: combination of parallel imaging with view sharing (TREAT). Invest Radiol 40:40–48

Gast KK, Viallon M, Eberle B et al. (2002) MRI in lung transplant recipients using hyperpolarized (3)He: Comparison with CT. J Magn Reson Imaging 15:268–274

Gast KK, Puderbach MU, Rodriguez I et al. (2003) Distribution of ventilation in lung transplant recipients: evaluation by dynamic 3He-MRI with lung motion correction. Invest Radiol 38:341–348

Gatehouse PD, Keegan J, Crowe LA et al. (2005) Applications of phase-contrast flow and velocity imaging in cardiovascular MRI. Eur Radiol 15:2172–2184

Gierada DS, Saam B, Yablonskiy D et al. (2000) Dynamic echo planar MR imaging of lung ventilation with hyperpolarized (3)He in normal subjects and patients with severe emphysema. NMR Biomed 13:176–181

Guenther D, Eberle B, Hast J et al. (2000) (3)He MRI in healthy volunteers: preliminary correlation with smoking history and lung volumes. NMR Biomed 13:182–189

Gust R, Kozlowski J, Stephenson AH et al. (1998) Synergistic hemodynamic effects of low-dose endotoxin and acute lung injury. Am J Respir Crit Care Med 157:1919–1926

Henderson AC, Ingenito EP, Salcedo ES et al. (2007) Dynamic lung mechanics in late-stage emphysema before and after lung volume reduction surgery. Respir Physiol Neurobiol 155:234–242

Heussel CP, Ley S, Biedermann A et al. (2004) Respiratory lumenal change of the pharynx and trachea in normal subjects and COPD patients: assessment by cine-MRI. Eur Radiol 14:2188–2197

Hogg JC, Chu F, Utokaparch S et al. (2004) The nature of small-airway obstruction in chronic obstructive pulmonary disease. N Engl J Med 350:2645–2653

Iwasawa T, Yoshiike Y, Saito K et al. (2000) Paradoxical motion of the hemidiaphragm in patients with emphysema. J Thorac Imaging 15:191–195

Iwasawa T, Kagei S, Gotoh T et al. (2002) Magnetic resonance analysis of abnormal diaphragmatic motion in patients with emphysema. Eur Respir J 19:225–231

Iwasawa T, Takahashi H, Ogura T et al. (2007) Correlation of lung parenchymal MR signal intensity with pulmonary function tests and quantitative computed tomography (CT) evaluation: a pilot study. J Magn Reson Imaging 26:1530–1536

Kauczor HU, Hofmann D, Kreitner KF et al. (1996) Normal and abnormal pulmonary ventilation: visualization at hyperpolarized He-3 MR imaging. Radiology 201:564–568

Lehmann F, Knitz F, Weiler N et al. (2004) A software tool for analysis and quantification of regional pulmonary ventilation using dynamic hyperpolarised-(3)He-MRI. Rofo 176:1399–1408

Ley S, Fink C, Puderbach M et al. (2004a) Contrast-enhanced 3D MR perfusion of the lung: application of parallel imaging technique in healthy subjects. Rofo 176:330–334

Ley S, Zaporozhan J, Morbach A et al. (2004b) Functional evaluation of emphysema using diffusion-weighted 3Helium-magnetic resonance imaging, high-resolution computed tomography, and lung function tests. Invest Radiol 39:427–434

Ley S, Puderbach M, Risse F et al. (2007) Impact of oxygen inhalation on the pulmonary circulation: assessment by magnetic resonance (MR)-perfusion and MR-flow measurements. Invest Radiol 42:283–290

Ley-Zaporozhan J, Ley S, Eberhardt R et al. (2007) Assessment of the relationship between lung parenchymal destruction and impaired pulmonary perfusion on a lobar level in patients with emphysema. Eur J Radiol 63:76–83

Ley-Zaporozhan J, Ley S, Kauczor HU (2008) Morphological and functional imaging in COPD with CT and MRI: present and future. Eur Radiol 18:510-21

Ley-Zaporozhan J, Puderbach M, Kauczor HU (2008) MR for the evaluation of obstructive pulmonary disease. Magn Reson Imaging Clin N Am 16:291–308

Loffler R, Muller CJ, Peller M et al. (2000) Optimization and evaluation of the signal intensity change in multisection oxygen-enhanced MR lung imaging. Magn Reson Med 43:860–866

Molinari F, Fink C, Risse F et al. (2006) Assessment of differential pulmonary blood flow using perfusion magnetic resonance imaging: comparison with radionuclide perfusion scintigraphy. Invest Radiol 41:624–630

Moonen M, Xu J, Johansson A et al. (2005) Effects of lung volume reduction surgery on distribution of ventilation and perfusion. Clin Physiol Funct Imaging 25:152–157

Morbach AE, Gast KK, Schmiedeskamp J et al. (2005) Diffusion-weighted MRI of the lung with hyperpolarized helium-3: a study of reproducibility. J Magn Reson Imaging 21:765–774

Morino S, Toba T, Araki M et al. (2006) Noninvasive assessment of pulmonary emphysema using dynamic contrast-enhanced magnetic resonance imaging. Exp Lung Res 32:55–67

Muller CJ, Schwaiblmair M, Scheidler J et al. (2002) Pulmonary diffusing capacity: assessment with oxygen-enhanced lung MR imaging preliminary findings. Radiology 222:499–506

Ohno Y, Chen Q, Hatabu H (2001) Oxygen-enhanced magnetic resonance ventilation imaging of lung. Eur J Radiol 37:164–171

Ohno Y, Sugimura K, Hatabu H (2003) Clinical oxygen-enhanced magnetic resonance imaging of the lung. Top Magn Reson Imaging 14:237–243

Ohno Y, Hatabu H, Higashino T et al. (2004a) Dynamic perfusion MRI versus perfusion scintigraphy: prediction of postoperative lung function in patients with lung cancer. AJR Am J Roentgenol 182:73–78

Ohno Y, Hatabu H, Murase K et al. (2004b) Quantitative assessment of regional pulmonary perfusion in the entire lung using three-dimensional ultrafast dynamic contrast-enhanced magnetic resonance imaging: preliminary experience in 40 subjects. J Magn Reson Imaging 20:353–365

Plathow C, Fink C, Ley S et al. (2004) Measurement of diaphragmatic length during the breathing cycle by dynamic MRI: comparison between healthy adults and patients with an intrathoracic tumor. Eur Radiol 14:1392–1399

Plathow C, Schoebinger M, Fink C et al. (2005) Evaluation of lung volumetry using dynamic three-dimensional magnetic resonance imaging. Invest Radiol 40:173–179

Rabe KF, Hurd S, Anzueto A et al. (2007) Global strategy for the diagnosis, management, and prevention of chronic obstructive pulmonary disease: GOLD executive summary. Am J Respir Crit Care Med 176:532–555

Ray N, Acton ST, Altes T et al. (2003) Merging parametric active contours within homogeneous image regions for MRI-based lung segmentation. IEEE Trans Med Imaging 22:189–199

Rosenkranz S (2007) Pulmonary hypertension: current diagnosis and treatment. Clin Res Cardiol 96(8):527–541

Salerno M, Altes TA, Brookeman JR et al. (2001) Dynamic spiral MRI of pulmonary gas flow using hyperpolarized (3)He: preliminary studies in healthy and diseased lungs. Magn Reson Med 46:667–677

Salerno M, de Lange EE, Altes TA et al. (2002) Emphysema: hyperpolarized helium 3 diffusion MR imaging of the lungs compared with spirometric indexes – initial experience. Radiology 222:252–260

Sandek K, Bratel T, Lagerstrand L et al. (2002) Relationship between lung function, ventilation-perfusion inequality and extent of emphysema as assessed by high-resolution computed tomography. Respir Med 96:934–943

Schuster DP, Marklin GF (1986) Effect of changes in inflation and blood volume on regional lung density – a PET study: 2. J Comput Assist Tomogr 10:730–735

Sergiacomi G, Sodani G, Fabiano S et al. (2003) MRI lung perfusion 2D dynamic breath-hold technique in patients with severe emphysema. In Vivo 17:319–324

Stadler A, Jakob PM, Griswold M et al. (2008) T(1) mapping of the entire lung parenchyma: Influence of respiratory phase and correlation to lung function test results in patients with diffuse lung disease. Magn Reson Med 59:96–101

Suga K, Tsukuda T, Awaya H et al. (1999) Impaired respiratory mechanics in pulmonary emphysema: evaluation with dynamic breathing MRI. J Magn Reson Imaging 10:510–520

Swift AJ, Wild JM, Fichele S et al. (2005) Emphysematous changes and normal variation in smokers and COPD patients using diffusion 3He MRI. Eur J Radiol 54:352–358

Swift AJ, Woodhouse N, Fichele S et al. (2007) Rapid lung volumetry using ultrafast dynamic magnetic resonance imaging during forced vital capacity maneuver: correlation with spirometry. Invest Radiol 42:37–41

Szilasi M, Dolinay T, Nemes Z et al. (2006) Pathology of chronic obstructive pulmonary disease. Pathol Oncol Res 12:52–60

Thabut G, Dauriat G, Stern JB et al. (2005) Pulmonary hemodynamics in advanced COPD candidates for lung volume reduction surgery or lung transplantation. Chest 127:1531–1536

van Beek EJ, Wild JM, Kauczor HU et al. (2004) Functional MRI of the lung using hyperpolarized 3-helium gas. J Magn Reson Imaging 20:540–554

Vonk Noordegraaf A, Marcus JT, Roseboom B et al. (1997) The effect of right ventricular hypertrophy on left ventricular ejection fraction in pulmonary emphysema. Chest 112:640–645

Vonk-Noordegraaf A, Marcus JT, Holverda S et al. (2005) Early changes of cardiac structure and function in COPD patients with mild hypoxemia. Chest 127:1898–1903

Weitzenblum E, Chaouat A (2005) Severe pulmonary hypertension in COPD: is it a distinct disease? Chest 127:1480–1482

Wild JM, Paley MN, Kasuboski L et al. (2003) Dynamic radial projection MRI of inhaled hyperpolarized 3He gas. Magn Reson Med 49:991–997

Woodhouse N, Wild JM, Paley MN et al. (2005) Combined helium-3/proton magnetic resonance imaging measurement of ventilated lung volumes in smokers compared to never-smokers. J Magn Reson Imaging 21:365–369

Zaporozhan J, Ley S, Gast KK et al. (2004) Functional analysis in single-lung transplant recipients: a comparative study of high-resolution CT, (3)He-MRI, and pulmonary function tests. Chest 125:173–181